ISTITUTO NAZIONALE DI FISICA NUCLEARE

Sezione di Milano

INFN/BE-00/02
8 Giugno 2000

PROPOSAL OF A HIERARCHICAL NEURAL SYSTEM FOR THE AUTOMATIC CLASSIFICATION OF MULTIDETECTOR ARRAY DATA

Monica Alderighi[1,2], Paolo Guazzoni[2,3], Stefania Russo[3], Giacomo R. Sechi[1,2], Luisa Zetta[2,3]

[1)] Istituto di Fisica Cosmica, CNR, via Bassini 15, 20133 Milano, Italy
[2)] INFN-Sezione di Milano, Dipartimento di Fisica dell'Universita', via Celoria 16, 20133 Milano, Italy
[3)] Dipartimento di Fisica dell'Universita', via Celoria 16, 20133 Milano, Italy.

Abstract

Biological vision processes are at the basis of many studies in the image-processing field. In this context, pre-attentive neural networks developed by S. Grossberg constitute an interesting approach. They are able to extract meaningful information from the global structure of data rather than from local relationships, yielding to a coherent and complete visual perception (emergent perception), also in case of noisy and incomplete images. The paper presents the application of Grossberg's approach to the analysis of scatter plots from nuclear physics experiments. The design and implementation of a pre-attentive neural system developed for this purpose are presented. Simulation results prove the goodness of the approach.

PACS: 07.05.Kf, 07.05.Mh

Published by ***SIS–Pubblicazioni***
Laboratori Nazionali di Frascati

1 INTRODUCTION

In Nuclear Physics at intermediate energy, preliminary analysis of experimental data is performed on 2-D histograms, or matrices, representing the measurement of some physical quantities of the reactions being studied. When visualized, these pictures contain clusters, each corresponding to a reaction product, that have to be extracted in order to obtain the necessary information for the identification of all detected ions.

In new generation multidetector arrays a great number, roughly thousands, of such matrices are typically produced. This makes the development of automatic analysis methods highly desirable.

Complexity of matrices does not favor the use of algorithmic approaches for the identification of clusters, since matrices are generally sparse and their data characterized by a low signal-to-noise ratio. They also show great variations of both point density and signal-to-noise ratio. Nevertheless, clusters can be easily perceived and recognized by sight. This has suggested using the same mechanisms that in biological visual systems allow for emergent perception, i.e. the extraction of hidden information that is present in a context but is not explicitly expressed.

Grossberg's work on this process yielded to the modeling of pre-attentive biological visual systems by means of hierarchies of artificial neural networks[1)-4)]. They are able to extract meaningful information from the global structure of data rather than from local relationships, giving rise to a coherent and complete visual perception, also in case of noisy and incomplete images. This approach has been widely and successfully used in the processing of SAR and satellite images[5)], but can also be of great interest in many other fields in which two-dimensional (2-D) representations, that can be considered as images, are used for data analysis.

The report is concerned with the application of Grossberg's approach to the analysis of scatter plots from nuclear physics experiments. To this purpose a pre-attentive neural system was designed and implemented using the Matlab language[6)]. This system was successfully employed for the analysis of CHIMERA experimental data[7), 8)]. Section 2 briefly reviews the experimental context of our application, while the main ideas at the basis of Grossberg's work are reported in Section 3. Section 4 describes the implemented system and discusses the results obtained. Finally, conclusions are drawn in Section 5.

2 EXPERIMENTAL CONTEXT

The study of nuclear multifragmentation obtained by heavy ion nuclear reactions has developed considerably in recent years. At the intermediate energy range ($10 \leq E \leq 100$ AMeV) reactions produce a great variety of particles and nuclei. Large multiplicities can be observed and the nature and energy of these products cover a considerable dynamic range. The improvements in detector techniques, electronic treatment of signals and computer power has led to the construction of extremely efficient devices that allow an almost complete detection and identification of these products.

Detection results are represented by means of 2-D histograms denoting the energy losses of particles in the detection cells. Each particle, or ion, is located at a point of the histogram depending on its nature (mass and charge) and velocity. Physical relationships among events are,

thus, expressed by topological relationships among the corresponding points in the histogram. Histograms can be filled by thousands of such events, some of them cumulating at the same location.

When sufficient statistics is collected, histogram visualization shows a picture of ridges (Z-lines) and valleys (Fig. 1(a)), each ridge corresponding to a given type of ion, mostly determined by its charge Z. In order to identify all detected ions, physicists have to recognize all the particles belonging to the same class, i.e. Z-line. In this sense, the identification problem becomes a classification problem.

Classification of Z-lines is generally performed manually. A human operator extracts, for each scatter plot, the points corresponding to each Z-line. The manual technique could be acceptable in old generation detectors, for which a low number of spectra were usually produced. Given the number of scatter plots now produced in a typical experiment (roughly thousands), automatic methods for data classification have to be investigated.

Many data classification methods have been described in the literature (see Benkirane et al.[9] for a detailed overview). These methods mostly consist in iterative minimization of some clustering criteria and imply the definition of a metric. The distance used for classification is a very important parameter and it is difficult to specify correctly in some applications. This holds true in our case. The high number of classes to be extracted and the variance of the number of events in each class may produce an undesired merging of two or more adjacent classes. For these reasons, standard classification methods are not adequate to solve our classification problem.

An alternative unsupervised method based on a sophisticated image segmentation algorithm was proposed[9], in order to overcome the limits of standard data classification algorithms. The method yields satisfactory results, but heavily relies upon the availability of a priori information concerning Z-line inter-distances and Z-line slopes at each point of the scatter plot matrix. Benkirane et al. describe how to obtain approximate values of these quantities, starting from the measurements of experimental energy losses reported with a precision of nearly 5% in the stopping power tables that can be found in the literature. These tables cannot be used directly for particle identification because of the non-linear behavior of CsI detectors, whose calibration function depends not only on particle energy, but on the particle's Z as well. The error in energy loss calculation with tabled data with respect to those experimentally measured is often over 20%. The effectiveness of this approach is, thus, limited to those cases in which a priori information can be reliably known.

3 GROSSBERG'S PRE-ATTENTIVE SYSTEMS

The synthesis of unambiguous global visual representation starting from ambiguous local information is a fundamental goal of visual science. Human observers often do not see images that are retinally present, and they often do see images that are not retinally present. Specifically, our percepts are not distorted by retinal veins, blind spot or retinal scotomas during normal viewing conditions, but are our visual processes to be adaptively designed to free our percepts from imperfections of our visual acquisition system. The same adaptive mechanism is

responsible for the generation of paradoxical percepts, well-known examples of which are the phenomena of Kanisza square[10], Da Vinci stereopsis[11], allelotropia[12], and equidistance tendency and Emmett's law[13,14].

Neurobiological processes located in the pre-attentive part of visual systems determine a large part of these phenomena. In this context, Grossberg's studies center on modeling autonomous massive parallel systems in order to capture and reproduce those mechanisms that make biological vision flexible and capable of abstraction. Grossberg's approach founds on mathematical analysis of biological visual systems described by means of differential equations, so as to investigate their emergent properties, that is those properties arising from global interactions and not only from local ones[15, 16]. This work has lead to the development of the FACADE (Form–And–Color–And–DEpth) theory[5, 17]. FACADE gives a unified explanation of many visual phenomena that may seem unrelated, explaining them all as manifestations of the mechanisms that, in the visual cortex, generate 3-D representations of boundaries and surfaces with which the visual world is perceived. The theory describes computational rules, that are to be applied in a prescribed order and that are naturally instantiated by neural processes.

The resulting neural system can be described in terms of two subsystems: the Boundary Contour System (BCS) and the Feature Contour System (FCS), which operate on boundary and surface representations respectively. In particular, the BCS generates emergent 3-D boundary segmentation that combines edge, texture, shading and stereo information. It is composed of a hierarchy of self-similar networks, each consisting of a particular kind of cells (simple, complex, hypercomplex, high-order hypercomplex, and dipole). Networks are characterized by ordered competitive and cooperative interactions across position, spatial frequency, orientation and disparity, which give rise to the coherent 3-D boundary segmentation that separate and complete the boundaries of objects.

The FCS discounts for illuminant and fills-in surface properties within FCS domains that are defined by BCS-FCS interactions. The FCS usually consists of networks characterized by diffusive interactions between neighboring cells, whose activity generates the feature filling-in over proper domains. This diffusive process across the cells is limited by the cells that correspond to the BCS boundary signals. These cells represent the barriers to the diffusive filling-in. From this point of view, a large class of visual illusions can be defined as unexpected combinations of BCS emergent segmentation and FCS filled-in surfaces.

FACADE pre-attentive networks model a set of general mechanisms that do not need statistical information about the external environment, neither in defining equations do include a priori information about the features of the objects to detect. Consequently they do not require learning.

Weight distribution is self-similar, i.e. all neurons share an identical structure (shape and values) for their receptive fields. Once determined the weight distribution of one neuron, the weight pattern of the whole network is given. Since our system deals only with the particular class of images represented by scatter plots, the adopted weight distribution need not to be of general use, but can be tailored to match specifically the required characteristics. Therefore, the employed distributions are much simpler than the structures proposed by Grossberg, resulting in smaller workloads and faster processing.

4. IMPLEMENTATION

The implemented system processes the data, in the form of (ΔE, L) matrices, from multidetector array data, and produces the related frequency identification spectrum in quasi-automatic way. ΔE represents the energy lost in the silicon detector, while L is the light output of CsI(Tl), corresponding to the remainder energy lost in the scintillator. In Fig. 1(a) a typical scatter plot for the reaction ^{108}Ag + ^{58}Ni, 52 AmeV[18] is shown.

The system is composed of two main parts. The first is neural and classifies the points in (ΔE, L) matrices as belonging or not belonging to a cluster. This is achieved by providing, as output, images in which clusters of points are replaced by strips, that is areas whose pixel values are set to "1" and matching the hyperbolic shape of the original clusters. The second part is based on procedural algorithms and applies an isomorphic transformation to produce 1-D frequency representations that are easier to interpret than original 2-D data representations.

At present, the neural processing is able to deal with image windows of 500 × 500 points, e.g. Fig. 1(b). Indeed, such windows were empirically found to contain sufficient information for classification and to show homogenous characteristics of their elements.

The implementation has been carried out using the Matlab language

4.1 Neural processing

The system is a hierarchical architecture consisting of two levels of neural networks. In the networks each neuron corresponds to a single pixel. Input and output images have the same dimensions, that is 500 × 500 pixels.

The first-level network performs an Adaptive Density Discrimination (ADD) of the original image window. Its output feeds the second-level networks, which realize an orientational completion of the determined structures by means of a Bipole Filter (BF) as neuron receptive field. These two levels implement a subset of the rules defined in Grossberg's BCS. It is to be noted that the proposed use of BCS rules differs from the classical one, in which these rules are applied for boundary detection. In fact, in order to make processing less sensitive to fluctuations shown by the local densities of data points, in our approach BCS rules are used to identify structures (clusters) as a whole, rather than their boundaries.

In our application clusters outline a hyperbolic shape with a slow evolving slope, showing a constant inclination angle in the 500 × 500 processing windows. In this way, in each window, they can be revealed as quasi-parallel strips.

The physically significant information to be revealed comes from the point density modulation that results in a picture of ridges and valleys. This is interpreted by the system as a 2-D spatial frequency distribution.

The ADD level, an on-center off-surround shunting network, performs a low-pass filtering of the input image, thus neglecting all frequencies higher than the ones defined in average by clusters, corresponding to noise. The equations defining the network are as follows:

$$\frac{d}{dt}x_{ij} = -\left(x_{ij} - E\right) + \sum_{(p,q)\in N_C}\left[\left(U - x_{ij}\right)C_{ijpq}\right]I_{pq} - \sum_{(p,q)\in N_S}\left[\left(x_{ij} + L\right)S_{ijpq}\right]I_{pq} \qquad (1)$$

where weight distributions for both excitatory and inhibitory inputs are normalized gaussian distributions:

$$C_{ijpq} = \frac{1}{2\pi\sigma_C^2}\exp\left\{-\frac{(i-p)^2+(j-q)^2}{2\sigma_C^2}\right\} \quad S_{ijpq} = \frac{1}{2\pi\sigma_S^2}\exp\left\{-\frac{(i-p)^2+(j-q)^2}{2\sigma_S^2}\right\} \tag{2}$$

For the properties of shunting networks[19), 20)], neuron activity x_{ij} always lies within the range [-*L*, *U*]. For *L* and *U*, the values 100 and 1 respectively were empirically determined. The widths of the two neighborhoods N_C and N_S, respectively center and surround, are determined by setting σ_C and σ_S. These values are defined for the ADD filtering operation to reveal the ridge/valley structure: σ_S is large enough to allow clusters to be perceived a single boundary structure; σ_C is smaller than σ_S in order to avoid spurious pattern detection, but also large enough to allow local density detection. Appropriate values of σ_C were determined as lying between the interval 3 and 5, while the value 10 for σ_S was generally used. Neuron output function is given by

$$g(v) = [v]^+ = \max\{v, 0\}. \tag{3}$$

As activity results, only the values calculated at the stationary state have been considered in simulations. *E* is the baseline activity value and *de facto* represents the threshold value of neuron activity. It was determined on the basis of the point density in the current image window. Different *E* values apply to different density conditions and signal-to-noise ratios. In this way, a single parameter allows to cope with varying image characteristics. As shown in Fig. 2(a), the ADD level is able to reveal the presence of clusters, but the resulting image contains incomplete and irregular strips. It is therefore necessary to smooth these structures in order to obtain complete filled strips matching the clusters.

The BF level accomplishes this by means of a number of additive networks that perform an oriented long-range cooperation between spatially separated cells placed along a selected direction, different for each network, yielding to the completion of the strips. To this end "bow-tie" shaped bipole fields filters have been defined as input receptive fields. Each orientation is obtained by properly rotating the filter mask. In our case, the completion has been realized only along the orientations associated to the strips. Because of the hyperbolic trend of clusters, these are restricted between 90° and 180°. Six networks have, thus, been implemented corresponding to the following six angles: 105°, 120°, 135°, 150°, 165° and 180°. The equations defining the networks are the following:

$$\begin{aligned} &\frac{d}{dt}z_{ij} = -z_{ij} + h\left(\sum_{(p,q)\in S_R} X_{pq}\, L^{R}_{(\beta,d)}\right) + h\left(\sum_{(p,q)\in S_L} X_{pq}\, L^{L}_{(\beta,d)}\right) \\ &h(v) = \frac{[v]}{\alpha + [v]^+} \quad f\left(z_{ij}\right) = \left[z_{ij} - A\right]^+ \end{aligned} \tag{4}$$

L^R and L^L identify the two lobes (respectively right lobe and left lobe) of the "bow-tie" mask. Two parameters are to be set to specify the bipole filter mask: the rotation angle (β) and the

distance (d) between the bipole cell and the two areas, S_R and S_L, covered by the mask lobes. The function h non-linearly compresses the value resulting from the separate convolution of the ADD output with the two lobes of the filter mask. In this way the bipole cell fires above threshold (A) only if sufficient inputs reach both lobes. For instance, in order for a horizontally oriented (180°) cooperative bipole cell to fire, both the left and right receptive fields of the cell need to receive excitatory stimuli from the ADD level. The α parameter controls the h function slope. The values for A and α were empirically determined and for the current application they were set to 0.2 and 0.30 respectively. f is the cell output function.

Fig. 2(b) shows the neural processing results for the image window in Fig. 1(b). The result of completion stage along three different directions is illustrated in Fig. 3. Among the possible six completion angles, the best fitting strip orientation in the selected window is β=165°. Fig. 3(b) shows the output of the network performing completion along this orientation. Fig. 3(a) and 3(c) display the completion along the two immediately adjacent orientations, respectively 180° and 150°. It can be noticed that these results are also valid from the classification point of view: strips are complete and not joining each other. The picture in Fig. 2(b) has been obtained by summing up the results for the three aforementioned orientations. This shows that an approximation of ±15° in the orientation choice is acceptable.

4.2 Post neural processing

This processing consists in a sequence of procedures that determine the borders of the strips identified in the neural stage, compute the central lines of filled strips (i.e. the Z-lines) and finally apply the linear isomorphism to the original data representation for final spectrum construction. The last step transforms the (ΔE, L) scatter plot to a new representation (L, ΔE), where the new coordinates of each point are obtained by applying the following rules[9]:

$$x_{new} = pos_1 + (pos_2 - pos_1)\frac{d_1}{d_1 + d_2} = pos_2 - (pos_2 - pos_1)\frac{d_2}{d_1 + d_2} \qquad (5)$$
$$y_{new} = L$$

For each point, d_1 and d_2 are the distances to the two nearest Z-lines, Z_1 and Z_2, while pos_1 and pos_2 are the intersections of Z_1 and Z_2 with the ΔE-axis in the original (ΔE, L) scatter plot. By the formula, Z_1 and Z_2 in the new representation are rendered as straight vertical lines located at the position pos_1 and pos_2. Clusters are vertically rectified as well. The frequency distribution spectrum is obtained by summing up, for each value of ΔE, the number of detected events for different values of E.

In Fig. 4(a) the central lines resulting for the window in Fig. 1(b) are highlighted. Fig. 4(b) displays the result of the coordinate linear transformation for the same window; the resulting 1–D spectrum is finally given in Fig. (5), which clearly shows the peaks corresponding to the different charges of the detected ions.

5 CONCLUSIONS

A system was developed and implemented for the automatic analysis of nuclear physics experimental data. The aim was to provide physicists data representations easier to interpret than original ones. Such experimental data are represented by means of 2-D matrices of isolated points, which gather in clusters corresponding to the physical classes to be identified. Given the sparsity nature of these matrices, classical clustering algorithms do not prove adequate.

In the proposed system this task is accomplished by a two-level neural system based on Grossberg's pre-attentive perceptive visual models, whose networks do not require learning. This neural stage translates the ridge/valley density modulation into a full/empty strip modulation. From these representations 1-D frequency distributions are easily derived by means of simple procedures.

The system semi-automatically processes scatter plot windows of 500×500 pixels and produces 1-D charge frequency distributions showing the peaks of detected ions. Results of simulations run on data coming from CHIMERA multidetector showed the effectiveness of the chosen approach, also in case of very noisy images[8)].

As future development of this work the processing of whole 4096×4096 scatter plots will be implemented.

6 REFERENCES

(1) S.Grossberg, Perc. and Psychophys. **41**, 87–158, (1987).
(2) S.Grossberg, Perc. and Psychophys. **55**, 48–120, (1994).
(3) S.Grossberg and E. Mingolla, Perc. and Psychophys. **38**, 141–171, (1985).
(4) S.Grossberg and L.Pessoa, Vision Research **38**, 2657–2684, (1998).
(5) S.Grossberg, E.Mingolla and J.Williamson, Neural Networks **8**, 1005–1028, (1995).
(6) M. Alderighi, P. Guazzoni, S. Russo, G.R. Sechi and L.Zetta, A pre-attentive neural system for the analysis of nuclear physics experimental data, accepted at the IEEE-INNS-ENNS International Joint Conference on Neural Networks, (Como, Italy, July 24-27, 2000).
(7) S.Aiello et al, Nucl. Phys. **A583**, 461–464, (1995).
(8) S.Aiello et al, A neural approach to the analysis of CHIMERA experimental data, in: Proc. of the International Conference on Computing in High Energy and Nuclear Physics (ed. M. Mazzuccato, February 2000), 41–44.
(9) A.Benkirane, G.Auger, D.Bloyet, A.Chbihi and E.Plagnol, Nucl. Instr. and Met. **A355**, 559-574, (1995).
(10) G.Kanisza, Italian Journal of Psychology **1**, 93–113, (1974).
(11) M.Kaye, Vision Research **18**, 1013–1022, (1978).
(12) H.Werner, Psychological Monograph **218,** whole No., (1937).
(13) W.C.Gogel, Psychonomic Monograph Supplement **3**, 153–169, (1970).
(14) D.Buckley, J.P.Frisby and J.E.W.Mayhew, Perception **18**, 563–588, (1989).
(15) M.A.Cohen and S.Grossberg, Transactions IEEE **SMC–13**, 815–126, (1983).
(16) S.Grossberg, Neural Networks **1**, 17–61, (1988).
(17) S.Grossberg, Mind and Language **5** (Special Issue on Understanding Vision), 411–456, (1990).
(18) INDRA–CHIMERA Collaboration – Private Communication.
(19) D.Levine and S.Grossberg, Journal of Theoretical Biology **53**, 341–380, (1975).
(20) S.A.Ellias and S.Grossberg, Biological Cybernetics **20**, 69–98, (1975).

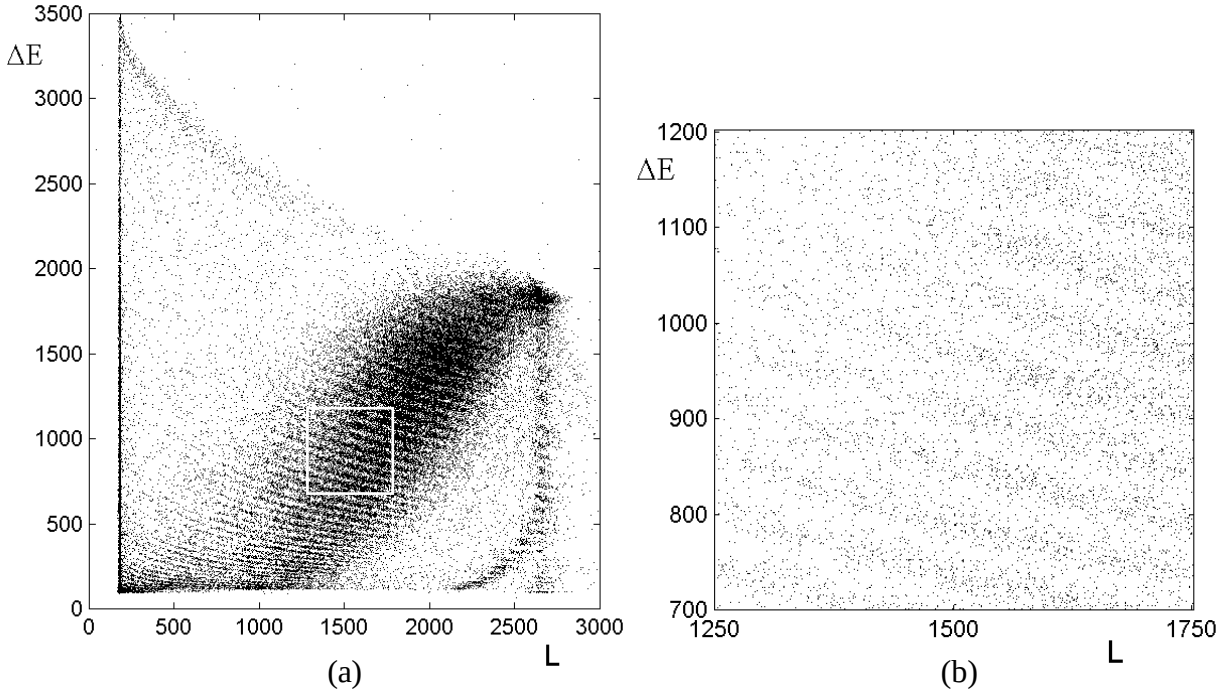

FIG. 1:(a) Input scatter plot for the reaction ^{108}Ag + ^{58}Ni, E=52 AMeV,
(b) selected processing window.

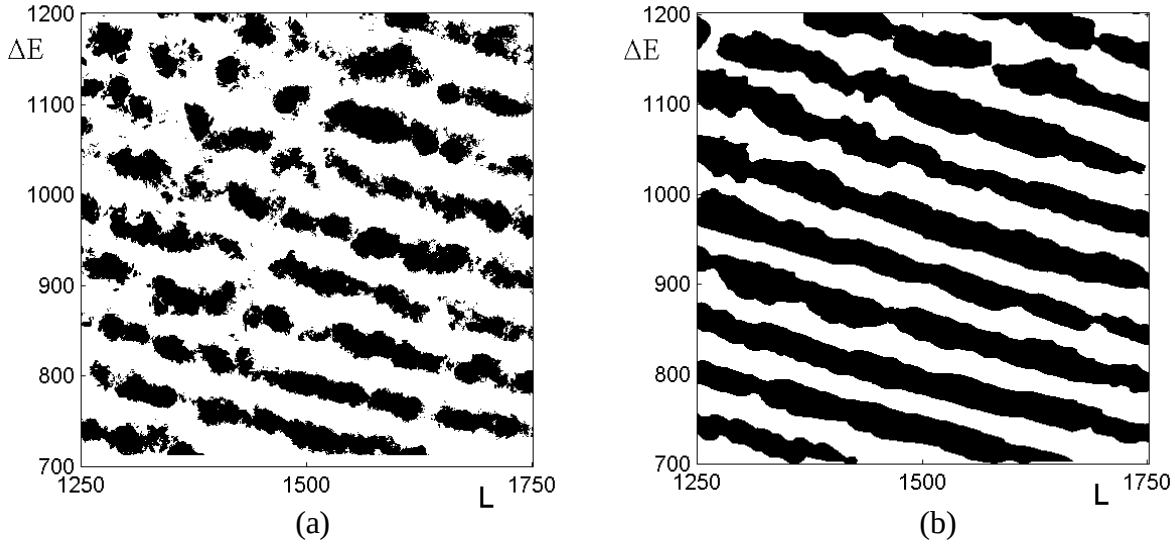

FIG. 2: (a) ADD level output,
(b) neural processing output.

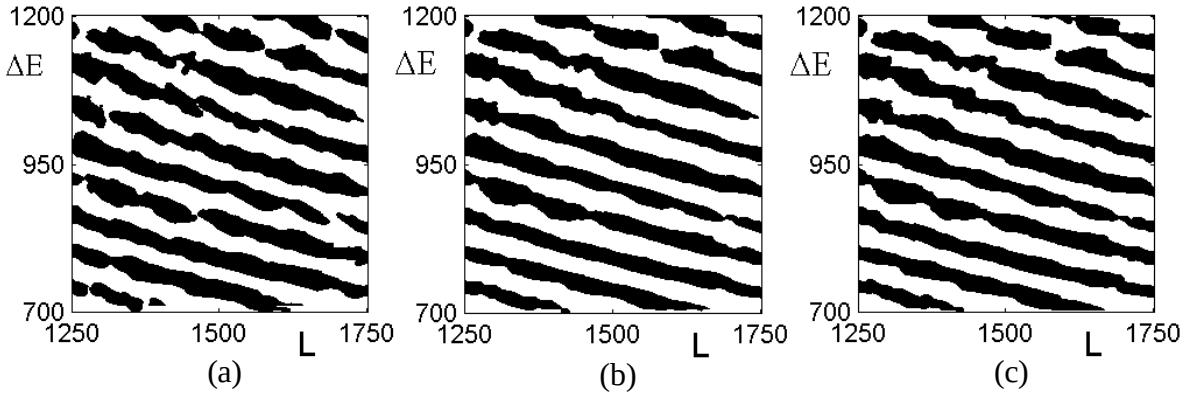

FIG. 3: BF results for three orientations of completion:
(a) 150°,
(b) 165°,
(c) 180°.

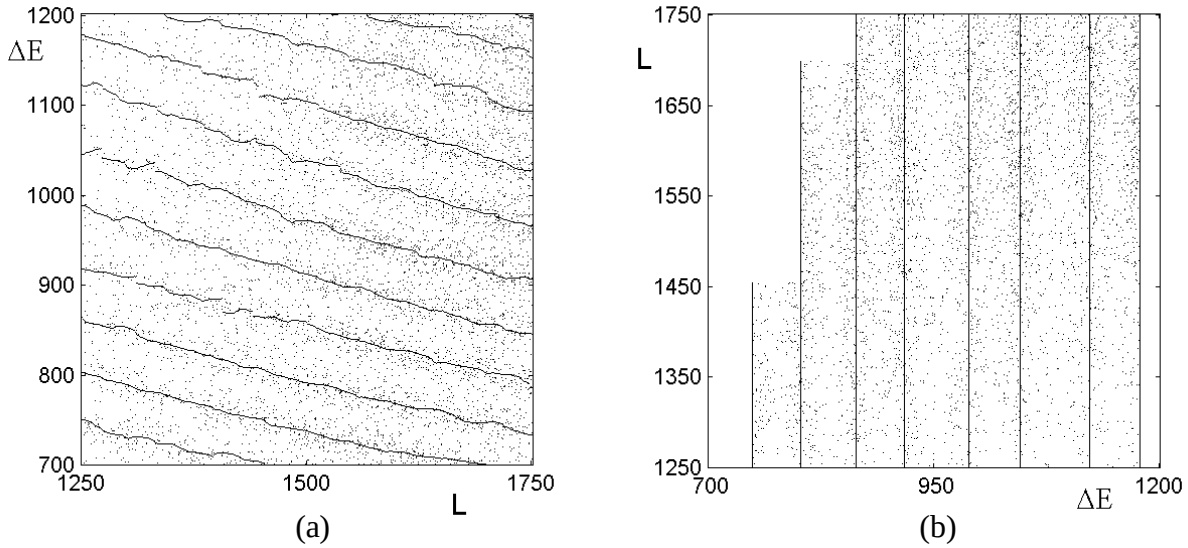

FIG. 4: Output of the post–neural processing:
(a) extracted central lines,
(b) coordinates linear transformation result.

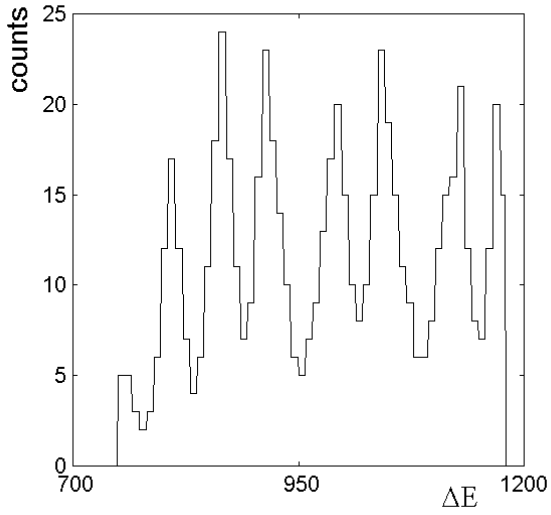

FIG. 5: Frequency distribution spectrum.